Management Strategies and Engineering Sciences 2027; 9(3):1-21

Evaluating Climate Uncertainty Effects on Optimized Cloud-Fog Configurations for Energy Management in Photovoltaic Buildings

Ahmed Kareem Alzeyadi[1], Hasan Ziafat[2*], Jafaar Fahad A.Rida[3], Mahdi Mosleh[1]

[1] Department of Computer Engineering, Isf.C., Islamic Azad University, Isfahan, Iran
[2] Department of Computer Engineering, Kas.C., Islamic Azad University, Kashan, Iran,
[3] Department of Communication Engineering, College of Engineering, University of Sumer, Dhiqar, Iraq

*** Corresponding author email address**: dr.ziafat@iau.ac.ir

Received: 2026-04-01 **Revised:** 2026-09-07 **Accepted:** 2026-09-15 **Initial Publish:** 2026-09-21 **Final Publish:** 2027-03-01

Abstract

This paper presents a novel cloud-fog computing framework for real-time energy management in building-integrated photovoltaic (PV) systems, addressing the critical challenges of operational uncertainty arising from dust-induced soiling and unpredictable cloud transients. The proposed architecture employs a Deep Deterministic Policy Gradient (DDPG) reinforcement learning agent operating within a hierarchical edge-cloud infrastructure that strategically distributes computational intelligence to balance latency constraints and processing demands. The framework integrates an adaptive thermal comfort model and a Prediction Interval Coverage Probability (PICP)-based uncertainty quantifier, formulating the optimization problem as a Markov Decision Process to enable holistic scheduling decisions that jointly optimize economic costs, occupant well-being, and system reliability. A dual-track learning mechanism, incorporating both global replay buffers and localized episodic memory, ensures rapid edge-level responsiveness while maintaining globally optimal scheduling capabilities. Experimental validation under two challenging scenarios heavy dust aggregation and persistent cloudy weather demonstrates significant performance improvements over traditional non-adaptive architectures. The proposed system achieved transmission latency reductions exceeding 54% at the fog layer and 30% at the cloud layer, maintained stable processing times despite fluctuating irradiance conditions, and delivered substantial energy savings, including a 51.4% reduction in cloud-layer energy consumption under data-intensive dusty conditions. These results establish the proposed framework as a scalable, energy-conscious, and resilient solution for smart building energy management, with future extensions envisioned for multi-agent coordination across microgrid networks and enhanced data privacy through federated learning approaches.

Keywords: *Cloud-fog architecture; Deep reinforcement learning (DDPG); Building energy management; PV uncertainty; Thermal comfort optimization; Edge computing; Microgrid resilience*

How to cite this article:

Kareem Alzeyadi, A., Ziafat, H., Fahad A.Rida, J., & Mosleh, M. (2027). Evaluating Climate Uncertainty Effects on Optimized Cloud-Fog Configurations for Energy Management in Photovoltaic Buildings. Management Strategies and Engineering Sciences, 9(3), 1-21.

1. Introduction

The accelerating transition toward low-carbon and decentralized energy systems has substantially increased the penetration of photovoltaic (PV) generation in residential, commercial, and smart-building environments. Building-integrated photovoltaic systems are particularly attractive because they transform building envelopes and rooftop areas into distributed generation assets while reducing dependence on conventional electricity sources and supporting broader urban decarbonization objectives. Nevertheless, the operational value of PV-based buildings depends not only on installed generation capacity but also on the ability of the energy management system to respond intelligently to highly dynamic environmental, electrical, computational, and occupant-related conditions. Recent research on resilient urban energy technologies has emphasized that renewable-energy selection and operation in buildings must account for uncertainty, robustness, and location-specific climatic conditions rather than relying exclusively on nominal generation potential [1]. This requirement is especially important in regions exposed to high solar irradiance but also to extreme environmental variability, where renewable-energy resources may be abundant while their usable output remains highly stochastic. Climate-related hazards can create cascading vulnerabilities in photovoltaic generation and thereby affect the reliability of the broader energy system [2]. Consequently, modern building energy management is evolving from conventional rule-based dispatch toward intelligent architectures capable of integrating renewable generation, energy storage, grid exchange, controllable loads, thermal comfort, uncertainty estimation, and computational resource allocation within a unified real-time decision framework.

A particularly important source of PV uncertainty is the interaction between atmospheric phenomena and module surface conditions. Dust accumulation can attenuate incoming radiation, alter optical transmittance, and progressively reduce the electrical output of PV modules, with the magnitude of degradation depending on dust composition, particle size, local meteorology, module inclination, humidity, and cleaning frequency. Early experimental evidence demonstrated substantial deterioration in photovoltaic performance following dust deposition and highlighted the importance of regional environmental characteristics in determining the severity of the phenomenon [3]. Similarly, experimental measurements of multicrystalline PV modules confirmed that accumulated dust can significantly reduce module performance and that site-specific soiling conditions must be considered when evaluating practical PV output [4]. The broader research literature has therefore recognized dust as a persistent engineering and maintenance challenge whose effects are governed by complex interactions among climate, surface properties, installation configuration, and cleaning practices [5]. Cloudiness creates a distinct but equally important uncertainty because changes in cloud cover can induce rapid and substantial irradiance fluctuations rather than the gradual degradation typically associated with soiling. Field evidence has demonstrated that cloud cover can sharply decrease photovoltaic power production and can interact with dust contamination to further compromise daily energy yield [6]. Experimental assessment of combined PV and solar-chimney operation under cloudy weather likewise illustrates the sensitivity of solar energy systems to rapidly changing atmospheric conditions [7]. More recently, extreme dust events have been shown to cause considerable reductions in regional photovoltaic potential, demonstrating that atmospheric dust should be treated not merely as a maintenance problem but also as an operational uncertainty requiring timely energy-management responses [8]. These findings collectively indicate that energy management strategies for PV-integrated buildings should simultaneously accommodate slow-changing soiling effects and fast cloud-induced transients rather than modeling either phenomenon as a static derating coefficient.

The technical behavior of a PV-based energy system is further complicated by the need to maintain efficient power conversion and grid interaction under such variable conditions. Photovoltaic arrays generally require DC–DC conversion and maximum power point tracking to continuously adjust their operating point as irradiance and cell temperature fluctuate. High-gain converter topologies have therefore been developed to improve voltage conversion performance and enhance the interface between renewable sources and downstream power-electronic stages [9]. Grid-connected PV systems also require reliable conversion from DC generation to synchronized AC output, with converter architectures playing a central role in maintaining voltage quality, frequency compatibility, and bidirectional energy exchange [10]. Grid-connected PV configurations based on boost-converter stages demonstrate the importance of coordinated converter control for efficiently extracting and transferring solar power [11]. Under partial shading, however, the power–voltage characteristic may exhibit multiple local peaks, making conventional maximum power point tracking less effective. Model-predictive approaches have therefore been adapted to improve global maximum power point tracking under partial shading [12], while hybrid metaheuristic MPPT techniques have demonstrated strong tracking performance under rapidly and gradually changing irradiance conditions [13]. These developments improve the local electrical efficiency of the PV subsystem, but they do not by themselves solve the broader system-level problem of coordinating PV production with battery scheduling, grid transactions, household demand, computation latency, and comfort constraints. Thus, converter-level intelligence must be embedded within a more comprehensive energy management architecture.

Battery energy storage systems provide a crucial degree of flexibility in this context by decoupling renewable generation from immediate consumption and enabling temporal energy arbitrage, peak reduction, resilience enhancement, and smoother grid interaction. However, the contribution of battery storage depends on its state of charge, charging and discharging efficiencies, degradation costs, operational limits, and coordination with other energy resources. Comprehensive analyses of battery energy storage in microgrids have emphasized that BESS applications should be selected and controlled according to technical, economic, and dynamic system objectives rather than treated as a homogeneous auxiliary component [14]. Accordingly, the energy management problem becomes inherently multi-objective: excessive charging and discharging can accelerate battery depreciation, excessive grid dependence can increase operating costs, aggressive load reduction can impair occupant comfort, and overly conservative control may waste available solar energy. Robust optimization has been proposed as one approach for microgrid energy management under uncertainty, particularly where generation and demand forecasts cannot be treated as perfectly accurate [15]. Likewise, real-time energy management based on deep reinforcement learning has demonstrated that adaptive agents can learn effective operational strategies directly from interaction with dynamic microgrid environments [16]. Deep reinforcement learning extends this concept by allowing control policies to adapt to nonlinear, continuous, and temporally coupled energy-management problems that are difficult to represent using fixed deterministic rules.

The growing application of artificial intelligence to energy management is supported by major advances in deep neural networks and sequential decision-making. Deep learning has enabled the extraction of complex nonlinear and temporal representations from large data streams, providing the methodological foundation for modern forecasting, anomaly recognition, and control applications [17]. In renewable energy systems, short-term multistep PV forecasting using deep-learning models can provide advance information about expected generation trajectories, which is particularly important for storage dispatch and demand-side scheduling [18]. Nevertheless, point forecasts alone cannot adequately represent the uncertainty surrounding future renewable generation. Prediction intervals offer a more informative representation by describing a plausible range around predicted values, and the statistical foundations of interval evaluation have long emphasized the joint consideration of coverage reliability and interval informativeness [19]. Contemporary renewable-energy forecasting research has consequently focused on neural-network-based prediction intervals that explicitly penalize excessive interval width while maintaining adequate coverage [20]. Such probabilistic information becomes particularly valuable when PV uncertainty arises simultaneously from clouds, dust, temperature, and other climatic factors. A recent bi-level framework for networked microgrids has further demonstrated how forecasting and uncertainty analysis can be embedded in an edge–fog–cloud architecture to improve hierarchical operational decisions [21]. The integration of uncertainty quantification with intelligent energy management therefore represents an important progression beyond deterministic scheduling.

At the same time, intelligent energy control increasingly depends on the Internet of Things and distributed computing because smart buildings generate continuous streams of data from irradiance sensors, smart meters, indoor environmental sensors, occupancy detectors, energy-storage controllers, and controllable appliances. Exclusive dependence on remote cloud computing can introduce communication delay, bandwidth consumption, and response-time limitations that are undesirable for time-critical physical control. Fog computing addresses these constraints by placing computation, temporary storage, filtering, and decision support closer to the physical devices. Cloud and fog layers can therefore be functionally differentiated: fog nodes respond rapidly to local events, whereas centralized cloud infrastructure performs computationally intensive learning, long-horizon optimization, and global coordination. Prior research on fog–cloud load balancing in smart grids has demonstrated that hybrid optimization can improve response and processing performance compared with conventional allocation strategies [22]. Efficient load balancing through coordinated fog and cloud computing can similarly improve smart-grid responsiveness and computational utilization [23]. Data-reduction methods based on clustering are also relevant because continuous IoT monitoring may generate substantial redundancy, and reducing unnecessary data transmission can lower communication and computation burdens in fog–cloud environments [24]. Resource-allocation methods specifically designed for fog-IoT environments further demonstrate that energy efficiency depends on effective assignment of devices, fog nodes, and computational resources [25]. Multi-agent and microservice-based approaches extend these principles by supporting dynamic scheduling, reliability, scalability, and more efficient resource utilization across distributed cloud–fog infrastructures [26].

Recent studies have increasingly coupled fog–cloud computing with machine learning, metaheuristics, and reinforcement learning to solve complex resource and energy-management problems. Hybrid machine-learning methods can improve energy-efficient task scheduling in IoT-based fog–cloud environments while satisfying quality-of-service constraints [27]. Metaheuristic task schedulers have likewise been developed to minimize energy consumption by assigning IoT workloads efficiently across computational resources [28]. Multi-objective optimization of computation offloading and task scheduling further demonstrates the need to jointly balance latency, energy use, and computational allocation in fog environments [29]. Within industrial energy systems, metaheuristic-optimized forecasting integrated into smart edge–fog–cloud frameworks has shown the value of combining distributed computation with predictive intelligence for energy monitoring and decision support [30]. Intelligent energy management systems can also integrate IoT, cloud and fog resources with advanced optimization to handle renewable intermittency, demand variability, and system operating constraints [31]. In parallel, deep reinforcement learning has been directly incorporated into cloud–fog energy management for interconnected microgrids, illustrating the potential of hierarchical architectures to support real-time decisions under renewable-generation uncertainty [32]. Graph-based and multi-agent reinforcement-learning approaches further indicate that distributed agents can coordinate complex network-level decisions, including reactive power optimization in active distribution systems [33]. Real-time optimal energy management under uncertainty has similarly benefited from deep reinforcement learning methods capable of learning adaptive policies without requiring a completely predetermined operating rule for every possible system state [34].

Despite these advances, a building energy management system cannot be evaluated solely according to electricity costs, photovoltaic yield, or computational efficiency because indoor environmental quality directly affects the primary users of the building. Heating, ventilation, and air-conditioning loads constitute a major component of building electricity consumption, yet rigid demand curtailment can produce unacceptable indoor conditions. Classical HVAC analysis has therefore incorporated thermal comfort prediction into system assessment and control [35]. Natural ventilation research in warm climates has additionally emphasized the complex interaction among energy efficiency, thermal comfort, heatwave resilience, and indoor air quality [36]. Adaptive comfort models provide a particularly appropriate basis for smart energy management because occupants can adapt physiologically and behaviorally to changing indoor and outdoor conditions, meaning that comfort should not necessarily be represented by a single invariant temperature set point. Adaptive predicted mean vote formulations were developed to improve the representation of thermal sensation by incorporating adaptive responses into conventional comfort assessment [37]. Integrating such comfort measures into energy-management objectives allows HVAC operation and controllable loads to be coordinated with PV generation, battery state, electricity price, and environmental uncertainty. Residential building energy-management frameworks incorporating rooftop photovoltaic generation have already demonstrated the importance of coordinating renewable supply and household energy use [38], but further integration with stochastic PV conditions, distributed computing, and adaptive machine intelligence remains necessary.

Another critical consideration is that the same distributed IoT infrastructure that improves energy awareness can introduce reliability, security, and architectural challenges. Fog and edge computing reduce dependence on distant cloud platforms, but the multiplication of sensing, communication, and computation nodes expands the operational complexity of the system. AI-enabled anomaly detection in fog–edge IoT environments demonstrates how distributed intelligence can enhance timely recognition of abnormal system behavior and improve cyber-resilience in data-intensive applications [39]. The general principle is directly relevant to intelligent energy systems, where incorrect sensor measurements, communication disruptions, or anomalous device behavior can compromise control decisions. Hence, the design of a cloud–fog building energy management framework should account not only for mathematical optimality but also for latency, local responsiveness, computational burden, scalable data handling, and system robustness. These issues become particularly significant when the system must respond to rapidly changing irradiance while simultaneously coordinating batteries, converters, loads, thermal conditions, and grid exchange. Consequently, an effective architecture requires a hierarchical division of responsibilities in which local or fog resources handle time-sensitive validation and response, while cloud resources undertake more computationally demanding policy learning, global optimization, and long-term memory management.

Although the literature has made substantial progress in PV forecasting, MPPT, battery scheduling, thermal comfort modeling, fog computing, and reinforcement-learning-based microgrid control, these research streams are frequently investigated in isolation. Existing studies have addressed the detrimental effects of dust and cloud cover on photovoltaic output [40], robust and intelligent microgrid energy management [15, 34], fog–cloud resource scheduling [25, 29], and probabilistic renewable forecasting [20], yet comparatively limited attention has been devoted to a unified building-level architecture that jointly treats dust-induced soiling and cloud transients as operational uncertainties while simultaneously optimizing electrical cost, battery behavior, controllable demand, thermal comfort, communication latency, and distributed computation. This gap is important because environmental and computational uncertainties are not independent in practical smart buildings: sharp irradiance changes may increase sensing and decision frequency, more intensive processing may increase communication loads, delayed cloud responses may undermine time-sensitive control, and inflexible demand actions may preserve electrical balance at the expense of occupants. Therefore, an integrated framework is required in which environmental sensing, probabilistic forecasting, edge-level responsiveness, cloud-based learning, energy-storage coordination, and occupant comfort operate as components of a single closed-loop control system rather than as disconnected optimization modules.

Accordingly, this study aims to develop and evaluate an uncertainty-aware cloud–fog energy management framework based on Deep Deterministic Policy Gradient reinforcement learning for building-integrated photovoltaic systems that jointly addresses dust accumulation and cloud-induced irradiance variability while optimizing real-time computational scheduling, energy costs, battery operation, grid interaction, and adaptive thermal comfort.

2. Methodology

This work proposes a cloud-fog-enabled building-integrated PV-battery system, architected to minimize total electricity costs—encompassing battery depreciation (C_1), PV investment (C_2), controllable appliance consumption (C_3), and thermal comfort deviation penalties (C_4)—while dynamically balancing generation, storage, grid exchange, and occupant well-being under highly uncertain climatic conditions. At the physical layer, the PV array is interfaced via an MPPT-based DC-DC boost converter, whose PI-based controller continuously adjusts the duty cycle to track the maximum power point despite fluctuating irradiance and temperature, with output power determined by panel area, irradiance, and efficiency. The DC power is then converted to grid-synchronized AC via a bi-directional DC-AC inverter (characterized in the d-q reference frame under SPWM control), which supplies household loads categorized as non-interruptible (NCHD) and interruptible (ICHD). A Battery Energy Storage System (BESS) is modeled with detailed state-of-charge (SOC) dynamics that account for charging/discharging efficiencies, leakage losses, and cycling-induced depreciation. On the demand side, thermal comfort is rigorously quantified via an adaptive thermal comfort (ATC) model derived from the Predicted Mean Vote (PMV) index, integrating indoor temperature, humidity, and occupant clothing insulation to ensure that the EMS actively penalizes deviations from the target comfort zone. To counter compounded forecasting errors from dust-induced soiling and stochastic cloud transients, a hierarchical sensing architecture relays real-time irradiance and soiling data to fog nodes for immediate MPPT/inverter adjustments, while the cloud-based EMS fuses this with indoor IoT data (temperature, humidity, occupancy) to evaluate thermal comfort. This enables multi-objective optimization of storage dispatch, grid exchange, and HVAC setpoints—for example, pre-cooling during cloud dips while preserving battery for peak tariffs—thereby maintaining both comfort and economic efficiency.

The energy management problem is cast as a Markov Decision Process (MDP) and tackled using the Deep Deterministic Policy Gradient (DDPG) algorithm, wherein the state variables—comprising net load, photovoltaic output, and real-time electricity pricing—inform the action policy covering generator dispatch, battery charge/discharge scheduling, and power exchanges with the grid, all with the objective of maximizing long-term cumulative rewards by curbing operational expenditures and constraint-related penalties. Within the proposed cloud-fog hierarchy, the fog tier assumes responsibility for live system monitoring, grid-connection verification, and temporary caching of transition samples, whereas the cloud tier undertakes the computationally heavy lifting of DDPG policy refinement, deriving optimal setpoints that are subsequently relayed downward via the fog layer to physical assets such as inverter controllers, battery management schedulers, and appliance switching mechanisms; concurrently, transition episodes are fed back to the fog to support continuous online retraining. This closed-loop, three-tiered architecture guarantees swift edge-level decision-making without sacrificing the globally optimal, comfort-conscious scheduling capabilities of the deep reinforcement learning agent. Finally, **Table 1** presents a detailed, step-by-step delineation of the proposed algorithm for managing the PV-integrated system under prevailing uncertainties.

Table 1. Steps of proposed algorithm to management of PV system under the uncertainty

Step	Layer	Procedure	Input ➔ Output
1	Cloud	Initialization – Set up the *DDPG* actor/critic networks, target networks, replay buffer, and long-term memory.	*Input*: Hyperparameters (γ, τ, buffer size). *Output*: Empty networks and buffer ready for training.
2	Physical + Fog	Sensing and Preprocessing – Read real-time PV irradiance, temperature, soiling, load demand, and indoor conditions. Correct PV power for dust/cloud losses.	*Input*: Raw sensor data. *Output*: Corrected PV power $P_{pv}(t)$, net load $P_d(t)$.
3	Fog	Islanding Check and State Packaging – Validate grid connection status (z_t). Combine all data into the state vector $S_t= [P_d, P_{pv}, P_{wt}, c^+, c^-]$. Send S_t and z_t to the Cloud.	*Input*: Grid status + physical data. *Output*: State vector S_t transmitted to Cloud.
4	Cloud	Action Selection (*DDPG*) – Pass S_t through the Actor network, add exploration noise, and generate the action vector $a_t= [P^i_{dg}, p_{ch}, p^d_{ch}, g^+, g^-]$.	*Input*: State S_t. *Output*: Optimal control actions (BESS power, grid trade, generation dispatch).
5	Cloud (Simulation)	Apply Actions and Compute Reward – Simulate BESS SOC dynamics, indoor temperature (HVAC), and power balance. Calculate the total cost (battery depreciation C_1, PV cost C_2, appliance penalty C_3, comfort deviation C_4, and grid cost). Set reward $r_t = -(C_1+C_2+C_3+C_4+C_{grid})$.	*Input*: Action a_t, current environment. *Output*: Next state S_{t+1}, reward R_t, updated SOC/temperature.
6	Cloud + Fog	Store Transition – Save the experience tuple (S_t, a_t, r_t, S_{t+1}) into the Cloud's replay buffer. Simultaneously, store it in the Fog's episodic memory for local retraining.	*Input*: Current transition. *Output*: Updated replay buffer and fog memory.
7	Fog	Constraint Validation and Actuation – Verify that the action respects SOC limits, inverter ratings, and power balance. If valid, send At to physical actuators (inverter, battery, switches). If invalid, apply a fallback heuristic (e.g., shed loads) and log the violation.	*Input*: Action a_t, physical limits. *Output*: Commands to hardware OR safe fallback action.
8	Cloud	*DDPG* Training (Episode End) – Sample a random mini-batch from the replay buffer. Update the Critic (minimize MSE loss) and Actor (policy gradient). Soft-update the target networks. Broadcast new policy weights back to Fog nodes.	*Input*: Batch of transitions. *Output*: Updated neural network weights for next episode.
9	Fog	Online Deployment – During live operation, Fog nodes run the latest policy locally (without noise) to make split-second decisions, while continuously feeding new rare/edge episodes to the Cloud for periodic fine-tuning.	*Input*: New incoming states. *Output*: Immediate real-time control commands.

The proposed cloud-fog energy management system executes a tightly sequenced 9-step pipeline as shown in Table 1: Step 1 initializes the cloud with DDPG actor-critic networks, target networks, and replay buffer; Step 2 performs physical and fog sensing to read real-time PV irradiance, temperature, soiling, and load data, correcting PV output for losses to compute net load; Step 3 validates grid connectivity at the fog layer, packages the state vector, and transmits it to the cloud; Step 4 passes this state through the actor network, injects exploration noise, and outputs optimal control actions for generation dispatch, battery cycling, and grid trading; Step 5 applies these actions in a cloud simulation that models battery SOC dynamics, indoor thermal evolution via an adaptive comfort model, and power balance, calculating the immediate reward and advancing to the next state; Step 6 stores the complete experience tuple simultaneously in the cloud's global replay buffer and the fog's episodic memory for dual-track learning; Step 7 enforces strict physical constraints at the fog layer—verifying SOC limits, inverter ratings, and power balance—dispatching valid commands to hardware actuators or applying a safe fallback heuristic when violations occur;

Step 8, at episode end, samples random mini-batches in the cloud, updates the critic via mean-squared error minimization and the actor via policy gradients, performs soft target updates, and broadcasts refined weights back to fog nodes; and Step 9 concludes the loop by having fog nodes deploy the latest policy locally and deterministically for split-second real-time control, while continuously feeding novel edge-case episodes upward for periodic cloud fine-tuning—ensuring rapid edge responsiveness alongside globally optimal, comfort-aware, and cost-efficient energy scheduling.

2.1. The Energy Management Problem

Properly characterizing the energy resources within a building constitutes an essential preliminary phase in designing an efficient Renewable Energy Management System (REMS). This section presents detailed models describing both the energy generation systems and controllable household devices in a smart building context. The core objective of the proposed REMS focuses on reducing the building's total electricity costs, formally defined by the following minimization function:

$$min\ F = C_1 + C_2 + C_3 + C_4 \qquad (1)$$

Where, C_1 is the lifetime depreciation cost of the energy storage system, C_2 is the investment cost of the PV system, C_3 is the cost of energy consumed by controllable appliances in the building, and C_4 is the cost associated with the deviation from the thermal comfort level of the building.

2.2. Model of the Battery

The state of charge (SOC) of the battery energy storage system (BESS) and its energy dynamics can be expressed as follows:

$$SOC(t) = E^{c}{}_{n}(t) / E_{n}^{c,rate} \qquad (2)$$

I.
$$E^{c}{}_{n}(t+1) = E^{c}{}_{n}(t) - \Delta t.\gamma^{d} P^{c}(t) - \left|P^{c}(t)\right|.\gamma^{c}\Delta t - E_{n}(t).\gamma\Delta t \qquad (3)$$

Where, E_n^{crate} is the rated energy capacity of the BESS, $E_n^c(t)$ is the energy stored in the BESS at time t, Δt is the duration of the scheduling interval, γ^c and γ^d are the charging and discharging efficiency factors, respectively, $P^c(t)$ and $P^d(t)$ are the charging and discharging power of the BESS at time t, γ^l is the leakage loss factor. The lifetime depreciation cost of the BESS is estimated as follows [25]:

$$C_1 = \beta.P^{c}(t).\Delta t + \beta E^{c}{}_{n}(t).\gamma\Delta t \qquad (4)$$

where β is the depreciation cost coefficient of the BESS.

2.3. Model of PV Power

A boost converter is employed as the DC-DC conversion stage to ensure continuous current operation in the inductor. The converter interfaces with the photovoltaic (PV) array through the array capacitance C_{pv}, forming a critical link in the power conditioning chain. The output characteristics of this interconnected system, representing the dynamic relationship between the PV array and the boost converter, are described in the Laplace domain by the following equation, which captures the essential behavior of the inductor current I_L in response to system variations.

$$I_{pv} = C_{pv} s U_{pv} + I_L \qquad (5)$$

Where I_L is the inductor current of the boost converter. The dynamic behavior of the DC-DC boost converter can be modeled using the average switching cycle model. When the capacitance C_{dc} and the inductance L_{dc} are sufficiently large, the average output voltage U_{dc} across the capacitor and the average output current I_{dc} through the inductor in the Laplace domain are given by equations (6) (7) [27]:

$$I_{dc} s I_L = U_{pv} - (1-D) U_{dc} \qquad (6)$$

$$C_{dc} s U_{dc} = I_{pv} - (1-D) I_L \qquad (7)$$

Where D is the duty cycle of the switch, which is controlled by the MPPT controller. The MPPT (Maximum Power Point Tracking) controller manages the switch to ensure that the PV array output voltage U_{pv} tracks the maximum voltage U_m, operating at the maximum power point. The controller's transfer function in the Laplace domain is represented as equation (8):

$$D = (k_p + \frac{k_i}{s})(U_m - U_{pv}) \qquad (8)$$

The parameters K_p and K_i represent the proportional and integral gains of the controller. Maintaining optimal PV system performance requires continuous operation at maximum power output, which is challenging given the variability of environmental conditions. As solar radiation, ambient temperature, and cell temperature fluctuate, the system's maximum power point shifts accordingly, necessitating effective tracking through maximum power point tracking (MPPT) algorithms. The instantaneous power output $P_{pv}(t)$ from the PV panels can be calculated based on the panel surface area A (m²), the solar irradiance k(t) (W/m²), and the conversion efficiency η, yielding the following relationship [14]:

$$P_{pv}(t) = Ak(t)\alpha \qquad (9)$$

The cost of the PV investment can be calculated as:

$$C_2 = C_{pv} = C_{ins} / (G^{\gamma} \times 365) \qquad (10)$$

In this equation, G_{γ} signifies the duration of the PV system's guaranteed operational life in years, and C_{ins} represents the aggregate installation expenses incurred by the user.

2.4. - Model of Controllable Devices

The DC-AC inverter constitutes the second critical stage of the power conversion process, responsible for transforming the direct current (DC) generated by the photovoltaic (PV) array into three-phase alternating current (AC) synchronized with the utility grid in both frequency and voltage amplitude. Its control architecture employs a dual-loop configuration that manages DC voltage regulation alongside reactive power control, while an integrated filtering stage actively suppresses harmonic distortions to maintain power quality standards. For power flow analysis applications, the inverter's power model is typically employed. Under sinusoidal pulse width modulation (SPWM) operation, the output voltage characteristics in the d-q reference frame are described by the following equations [29]:

$$u_{id} = \frac{U_{dc}}{2U_p} u_{rd} \qquad (11)$$

$$u_{iq} = \frac{U_{dc}}{2U_p} u_{rq} \qquad (12)$$

In the inverter modeling framework, u_{id} and u_{iq} represent the d-axis and q-axis components of the inverter's output voltage, while u_{rd} and u_{rq} denote the corresponding components of the modulation wave voltage, with U_{dc} being the DC link voltage and U_p representing the peak value of the carrier wave, together providing an accurate characterization of inverter behavior under sinusoidal pulse width modulation (SPWM) control for seamless PV system integration. Complementing the physical modeling, controllable household devices are classified into two distinct categories: Non-interruptible Controllable Household Devices (NCHD), such as tea makers, which must complete their operation cycle once initiated, and Interruptible Controllable Household Devices (ICHD), like washing machines, which can be paused and resumed at any time. Regarding power consumption characteristics, ICHDs consume no power when switched off and draw their rated power (P^{IcHD}_{rate}d) during operation, whereas NCHDs continue to consume a baseline amount, termed base power ($P^{NcHD}_{\beta ase}$), even when interrupted, leading to the following expression for total power consumption (C^{c}_{on}) by both device types:

$$C_3 = C_{con} = \begin{cases} P^{rate}_{ICHD} & if \quad on \\ P^{rate}_{NCHD} & if \quad on \\ P^{0}_{ICHD} & if \quad \text{int}\, errupted \\ P^{0}_{NCHD} & if \quad \text{int}\, errupted \end{cases} \qquad (13)$$

2.5. - Prediction interval coverage probability (PICP)

This reliability index, which evaluates the percentage of actual observations captured within the PIs, is known as the Prediction Interval Coverage Probability and is defined as:

$$PICP = \frac{1}{N}\sum_{i=1}^{N} 1 \qquad \hat{l}_i \le y_i \le \hat{u}_i \qquad (14)$$

The indicator function 1(A) returns one when event A happens and zero when it does not, with the PICP ideally matching the predefined PI confidence level. As for interval sharpness, it is measured by the average width computed over the entire sample set, a metric termed the Prediction Interval Average Width.

$$PIAW = \frac{1}{N}\sum_{i=1}^{N} w_i \qquad (15)$$

Furthermore, a scale-invariant variant of the PIAW exists, referred to as the Prediction Interval Normalized Average Width (PINAW), which effectively neutralizes the effect of the target variable's range, and is given by:

$$PINAW = \frac{1}{NR}\sum_{i=1}^{N} w_i \qquad (16)$$

where R= $y_{max} - y_{min}$ indicates the target variable's range, computed as the difference between the maximum and minimum values of y, ensuring the PINAW scale is between 0 and 1. As an evaluation tool, the Winkler score simultaneously accounts for both the precision (sharpness) and the correctness (reliability) of prediction intervals with respect to the target coverage probability. Notably, when the intervals are equal-tailed, this measure is directly analogous to the pinball loss; hence, a lower score signifies that the predicted endpoints accurately approximate the desired quantiles. Since the raw score remains sensitive to the scale of the data, a scale-invariant normalized form is frequently employed to ensure fair and comparable assessments across different datasets.

2.6. - Thermal Comfort Model

To achieve a more accurate representation of thermal comfort, a model must account for variables beyond indoor temperature, including occupant clothing insulation and humidity levels. This research adopts an adaptive thermal comfort (ATC) approach, where the comfort level at time t is mathematically represented by equation (17). In this formulation, α denotes an adaptation coefficient, while PMV refers to the Predicted Mean Vote index, a standardized metric for assessing thermal sensation [32-33].

$$ATC(t) = PMV(t) / 1 + \alpha PMV(t) \qquad (17)$$

where α denotes the adaptation coefficient, while the Predicted Mean Vote (PMV) serves as the metric for assessing thermal comfort levels. The mathematical formulation for PMV is given as [34]:

$$C_4 = PMV(t) = X.T_{ID}(t) + Y.H_o(t) - Z \qquad (18)$$

The PMV value is calculated using equation (18), where the parameters X, Y, and Z are coefficients that vary according to the clothing insulation level of the building occupants. The variables TID(t) and Ho(t) correspond to the indoor temperature and indoor humidity at time t, respectively. Within the overall optimization framework, the term C_4 represents the cost associated with deviations from the target thermal comfort level, which is derived directly from the calculated ATC(t) value.

3-1 - Cloud-fog-computing for the PV system based on Reinforcement Learning

To address real-time parameters and inherent uncertainties, the Energy Management System (EMS) problem is modeled as a Markov Decision Process (MDP). In this formulation, the state variable for microgrid n at time t, denoted as s_{nt}, is expressed as:

$$s_{n,t} = [P_d(t), P_{pv}(t), P_{wt}(t), c_t^+, c_t^-] \qquad (19)$$

The state representation comprises three primary components: the net load Pd(t), the combined power generation from photovoltaic $P_{pv}(t)$, and the dynamic pricing signals for grid electricity exchange, specifically buying costs (c_t^+) and selling revenues (c_t^-). The corresponding action variable for microgrid n at time t, a_{nt}, is defined by:

$$\alpha_{n,t} = [P_{DG}^i(t), P_{m,t}^c(t), P_{m,t}^d(t), g_t^+, g_t^-] \qquad (20)$$

The action set a for microgrid n at time t consists of the controllable generator output $P^{iDG}(t)$, the BESS charging/discharging powers ($p^c_{m,t}$ and $p^d_{m,t}$), and the bidirectional power exchange with the utility grid (g_t^+ for purchases, g_t^- for sales). The reward function assigned to microgrid n is expressed as:

$$r_{n,t} = \omega_1(-(\sum_i^D (f_{DG}^i(t) + C_m(P_{m,t}^c, P_{m,t}^d) + C_{grid})) - \omega_2 C_{EMS} \qquad (21)$$

In this formulation, ω_1 and ω_2 serve as weighting factors that adjust the contribution of each term to the overall reward. By seeking to maximize the cumulative reward over time, the optimization effectively pursues the minimization of total operating expenses comprising dispatchable generation costs, battery degradation from cycling, and grid transaction costs along with any constraint violation penalties denoted as C_{EMS}.

The proposed cloud-fog framework operates through a systematic multi-step process designed for efficient real-time energy management of PV farms. Firstly, for a defined planning horizon (T), the complete state space of each PV farm is established as S = {s_{1t}, s_{2t}, …, s_{nt}}, where each state vector encompasses critical parameters including net load, PV power output, real-time electricity prices, and other relevant operational data. This comprehensive state representation forms the foundation for subsequent decision-making. In the second step, all generated state information is transmitted to the fog layer, which serves as an intermediary processing unit. Upon receiving this data, the fog layer performs real-time monitoring and verification of the binary islanding event status for each PV farm, denoted as {z_{1t}, z_{2t}, …, z_{nt}}. This critical check determines whether each PV farm is operating in grid-connected mode or has been isolated due to disturbances or maintenance requirements. The fog layer's real-time processing capability enables immediate detection of such events, ensuring rapid response to changing grid conditions [39]. Finally, after processing and validating the information at the fog layer, all consolidated data including both the original state information and the islanding status indicators is transmitted upward to the cloud layer. This centralized cloud infrastructure houses the reinforcement learning algorithms, specifically the DDPG agent, which utilizes the comprehensive dataset to compute optimal control actions [40]. This hierarchical information flow ensures that while real-time monitoring and preliminary processing occur at the edge through the fog layer, the computationally intensive deep learning-based optimization is performed in the cloud, achieving both responsiveness and analytical power in the energy management system.

$$Fog_n : s_{n,t} = [P_d(t), P_{pv}(t), P_{wt}(t), c_t^+, c_t^-] \qquad (22)$$

The third step represents the core computational phase where the deep reinforcement learning engine is activated to solve the energy management optimization problem. Upon receiving the consolidated information from the fog layer including the complete state space S = {s_{1t}, s_{2t}, …, s_{nt}} and the real-time islanding status indicators {z_{1t}, z_{2t}, …, z_{nt}} this data is immediately stored in the environment space of the cloud platform. The environment space serves as a structured repository that maintains the current operational context of all PV farms, effectively capturing the dynamic conditions under which the energy management decisions must be made. With the environment properly initialized, the DDPG (Deep Deterministic Policy Gradient) algorithm is triggered, leveraging its actor-critic architecture to process the incoming state information. The actor network evaluates the current state to generate optimal actions, while the critic network assesses the quality of these actions by estimating their long-term value. Through this integrated approach, the reinforcement learning framework systematically explores the action space to identify control strategies that minimize operational costs while respecting all system constraints, ultimately computing the action space A = {a_{1t}, a_{2t}, …, a_{nt}} and corresponding reward function R = {r_{1t}, r_{2t}, …, r_{nt}} that will be transmitted back through the fog layer for implementation at the physical device level.

$$s_t = \sum_n s_{nt} \tag{23}$$

In the agent duty within the DDPG framework, the subsequent step involves calculating the action space A = {a_{1t}, a_{2t}, …, a_{nt}} and the corresponding reward function R = {r_{1t}, r_{2t}, …, r_{nt}} at the cloud layer. These outputs represent the optimal control decisions for each PV farm and the immediate feedback on their performance, respectively. For the cloud layer output, we have the following formulation that captures the complete set of decisions and their evaluated outcomes, which are then transmitted back to the fog layer for implementation and storage in the dedicated memory datasets of each PV farm.

$$Cloud \quad layer \quad output: \begin{cases} a_{1t}, a_{2t}, \dots, a_{nt} \\ r_{1t}, r_{2t}, \dots, r_{nt} \end{cases} \tag{24}$$

In the fifth step, the transition episodes consisting of (a_t, r_t, s_t, s_{t+1}) for each PV farm are transmitted from the cloud layer back to the fog layer, where they are systematically stored in dedicated memory datasets specifically curated for the Basra city climate conditions. The hardware configuration shown in **Figure 2** includes a DC-DC booster, a DC-AC inverter employing SPWM that routes grid load back to the inverter, and a buck-boost converter linked to the BESS to support both discharging and charging functions. A distinct BESS pathway receives supervisory commands from the cloud layer, which serves as the primary decision-making authority within the proposed system. While the system operates amidst the two prevailing uncertainties—dust accumulation and cloud-induced variability—the DDPG framework executed at the cloud layer derives the action and its associated reward function. Concurrently, the building's thermal comfort requirements are assumed to be monitored via IoT devices used by occupants, enabling them to send preference commands to the fog layer, where these requests are reconciled with the control signals produced by the DDPG computations. By preserving these episodes in the fog layer's short-term memory, the framework enables continuous learning and adaptation, as these stored transitions can be periodically sampled to retrain and refine the DDPG agent, ultimately improving the energy management system's performance under the specific climatic and operational conditions of Basra.

$$D = \begin{cases} MG_1(e_{11}, \dots., e_{M1}) \\ MG_2(e_{12}, \dots., e_{M2}) \\ \vdots \\ MG_n(e_{1n}, \dots., e_{Mn}) \end{cases} \tag{25}$$

Upon successful verification of the control actions (a_{1t}, a_{2t}, …, a_{nt}), the command signals are transmitted through the fog layer to the physical devices. Concurrently, critical decision variables, including $P^i_{DG}(t)$, $p^c_{m,t}$, $p^d_{m,t}$, and grid exchange parameters g_t^-, g_t^+, are committed to the cloud's long-term repository. If the operational constraints are not satisfied, the system triggers a recursive loop to the initial stage of the algorithm.

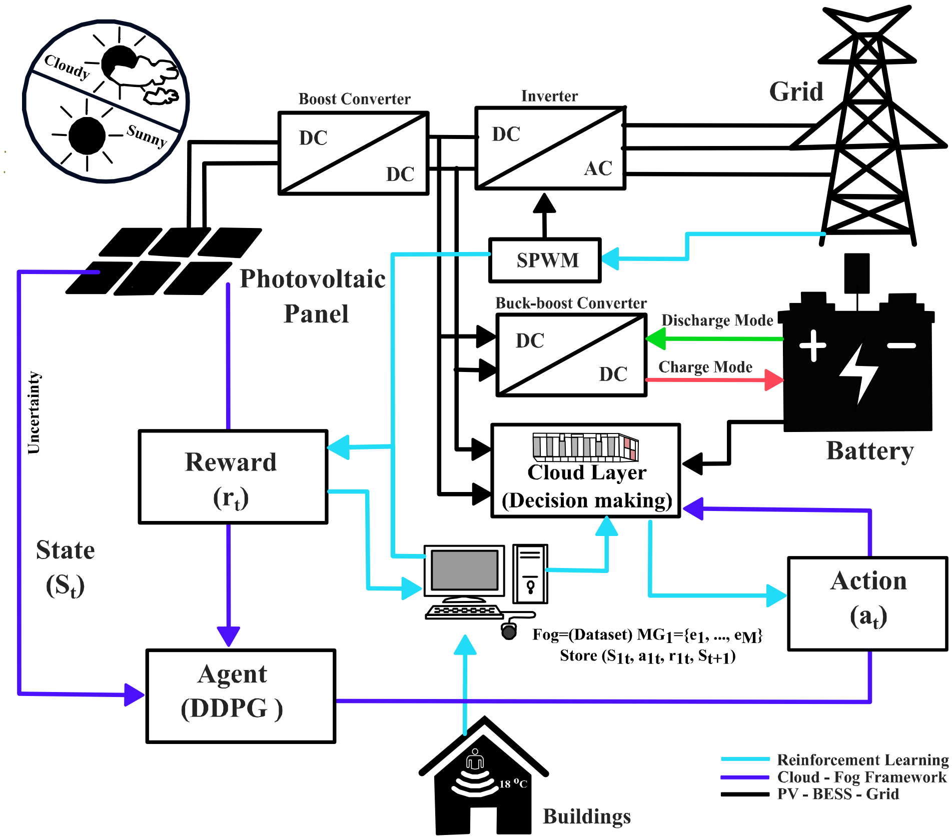

Figure 1. Proposed reinforcement-learning-based cloud-fog framework for building-integrated PV under uncertainty.

3-2 - Definition of Scenarios

The scenario framework addresses the unpredictability of dust build-up on PV panels, variability in cloud cover, and the interplay between these two factors. The primary contributors to dust soiling on photovoltaic surfaces can be grouped into four main categories: climatic conditions, environmental pollutants, site selection, and the PV system's own material characteristics. Climatic drivers like dust storms, wind velocity, and atmospheric pressure, combined with environmental contaminants such as airborne particulates, bacteria, carbon residues, and clay minerals, collectively intensify the soiling effect. For the first scenario, a 20-day data collection period was established, assuming a steady ambient dust concentration of 150 µg/m³ and a deposition velocity of 0.012 m/s for 10 µm particulates on a panel inclined at 25°. This results in an initial soiling rate of roughly 15.5 mg/m² per day, prior to any corrections for wind and humidity. Since rain and windy conditions are excluded, the average net accumulation over this 20-day dry interval equates to 10.2 mg/m² per day. Conversely, the second scenario omits dust deposition entirely, concentrating solely on cloudy weather conditions; here, a global irradiance value of 5.26 kWh/m² is applied to determine the available solar energy reaching the surface in Basra's climate.

3. Findings and Results

4-1 - Robustness Analysis

Figure 2 presents a comparative evaluation of data transmission latencies across both the cloud and fog computing layers, assessed under the two distinct scenarios outlined earlier. The core distinction between the two architectures lies in their operational logic: the traditional cloud-fog model operates without any adaptive learning mechanisms, whereas the proposed framework integrates a reinforcement learning (RL) agent, which is specifically designed to dynamically optimize data routing, scheduling, and offloading decisions in real time. In the first scenario—which focuses exclusively on the unpredictability caused by dust aggregation on PV surfaces—the cloud-layer transmission times for the conventional and proposed systems are recorded at 186.50- and 130.4-time units, respectively. This translates to a notable reduction of approximately 30% when reinforcement learning is applied. For the fog layer under the same dusty conditions, the traditional approach yields a transmission time of 27.61, while the RL-enhanced method significantly lowers this to just 12.45—an improvement of over 54%, highlighting the particular effectiveness of the proposed algorithm in edge-level processing. Shifting to the second scenario, which simulates persistent cloudy weather conditions, the cloud-layer transmission times measure 169.3 for the baseline architecture and 110.2 for the RL-driven counterpart. Meanwhile, in the fog layer under these overcast conditions, the conventional model registers 50.90, whereas the proposed method achieves a substantially lower value of 25.07. Overall, these findings clearly demonstrate that the reinforcement learning mechanism consistently outperforms the traditional approach across all layers and environmental conditions. It is also worth noting that the cloudy weather scenario generally exhibits higher fog-layer latencies (50.90) compared to the dust-aggregation scenario (27.61) in the traditional setup—likely due to fluctuating irradiance levels and variable data loads that complicate edge processing. Nevertheless, the proposed RL framework proves remarkably robust, cutting fog-layer transmission times by nearly half even under these more demanding meteorological circumstances, thereby validating its potential for enhancing real-time PV system monitoring and control in resource-constrained environments.

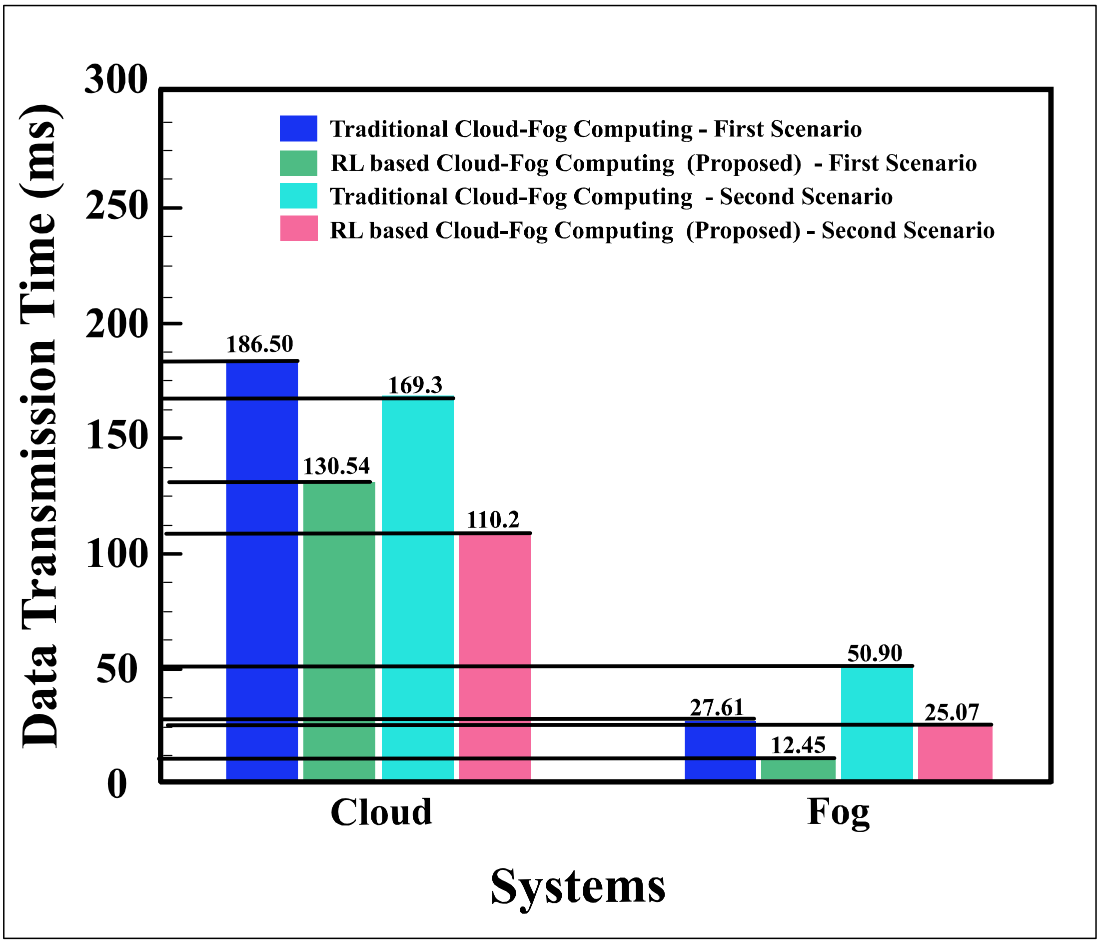

Figure 2. Cloud and fog of data transmission time for both scenarios

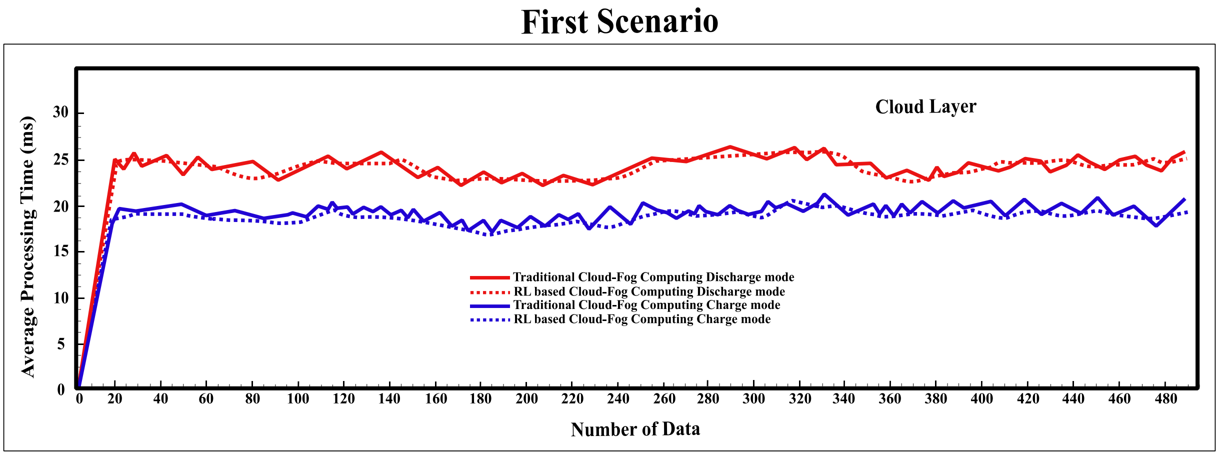

(a)

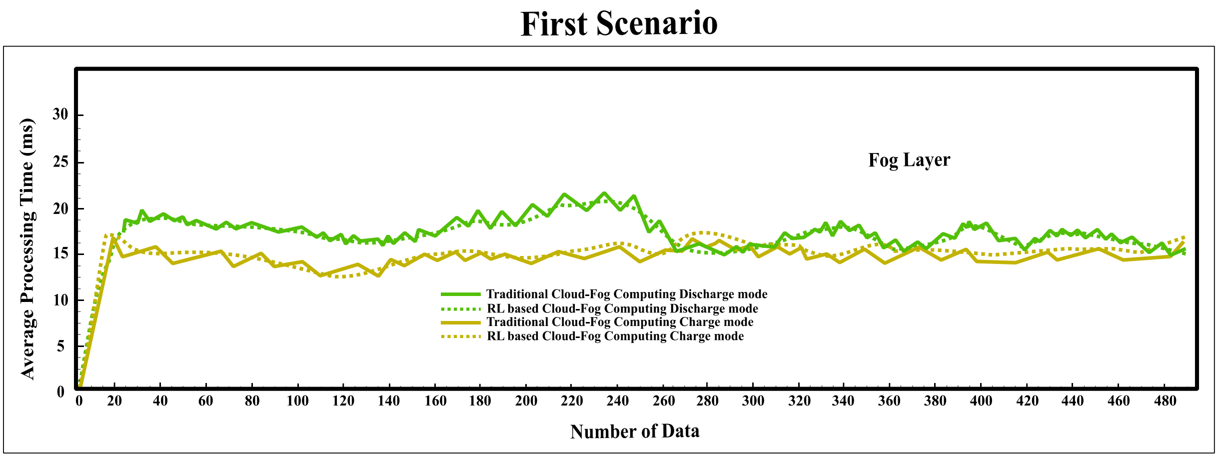

(b)

Figure 3. Average processing time variation for the fog and cloud layers, comparing the proposed algorithm and the traditional algorithm in the first scenario.

Figure 3 compares the average processing times of the fog and cloud layers for the proposed algorithm versus the traditional method under the first scenario, which involves dust accumulation. In this case, the conventional system produces considerably sharper spikes, causing erratic data transmission that can delay DC-AC inverter voltages during the charging phase. The proposed PV-optimized system, however, mitigates these fluctuations and ensures smoother data transfer, thanks to the optimization benefits of its actor-critic mechanism. Specifically, during discharge/charge data transfers, the fog layer temporarily stores transition samples (states, actions, rewards) and relays them to the cloud for DDPG policy updates; the cloud then handles the intensive computations to generate optimal charge/discharge setpoints, sending these commands back through the fog to the physical battery schedulers, while simultaneously feeding new transition episodes upward to support ongoing online retraining for future scheduling adjustments.

A similar comparison for the second scenario is presented in Figure 4, which again shows that the traditional approach exhibits more prominent spikes than the proposed algorithm for both layers. When contrasting the two figures, it is evident that the average processing times for both the cloud and fog are higher in the second scenario—approximately 35 ms and 27 ms, respectively, compared to 26 ms and 22 ms in the first scenario. This increase highlights that dust accumulation on PV panels introduces persistent uncertainties and time-dependent instability, though these issues can be addressed through various mitigation strategies. Furthermore, across both Figure 3 and Figure 4, the discharge mode consistently yields higher average values, as it involves more intricate data handling due to simultaneous commands from the grid and internal coordination between the DC-DC and DC-AC inverters.

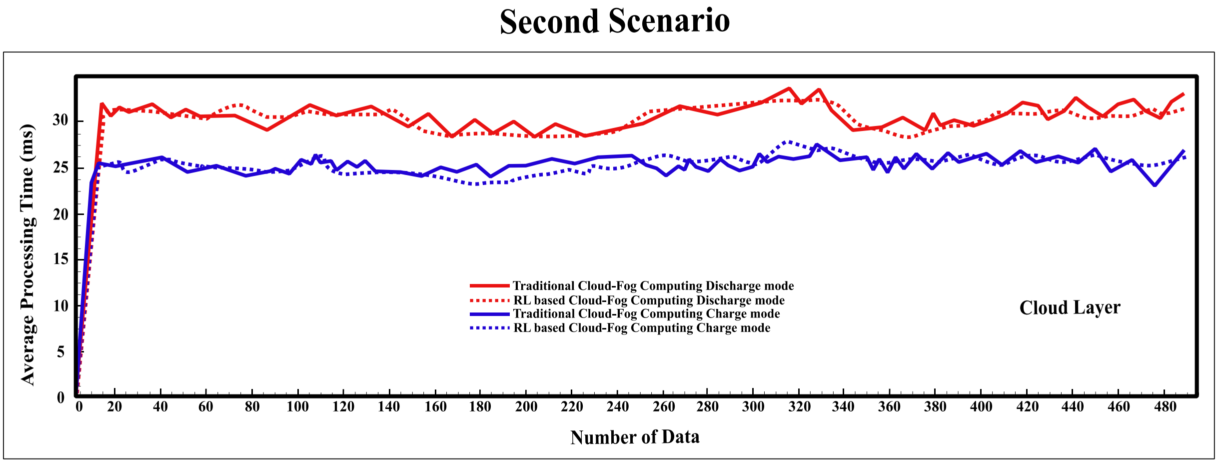

(a)

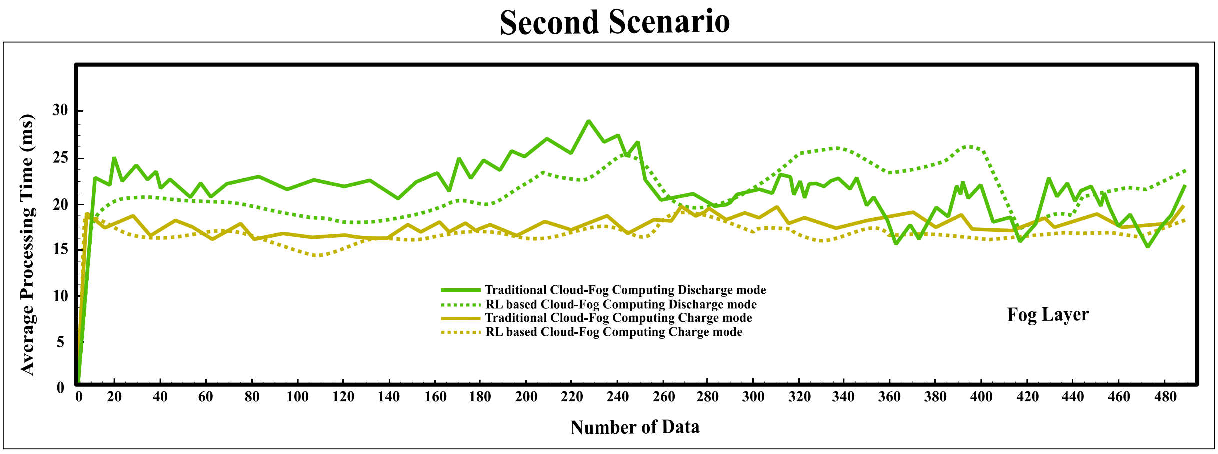

(b)

Figure 4. Average processing time variation for the fog and cloud layers, comparing the proposed algorithm and the traditional algorithm in the second scenario.

4-2 Energy Consumption Analysis

Figure 5 presents a comparative analysis of energy consumption (measured in megajoules, MJ) across both the fog and cloud computing layers, evaluating the performance of the proposed system against the traditional approach under two distinct operational scenarios (Scenario 1 and Scenario 2). Beginning with the cloud layer, the proposed system consistently achieves notable energy savings. In Scenario 1, the traditional system consumes 1.07 MJ, whereas the proposed system drastically reduces this to just 0.52 MJ—marking a substantial reduction of approximately 51.4%. For Scenario 2, the energy footprint for both systems declines overall, with the traditional system consuming 0.80 MJ and the proposed system consuming 0.71 MJ. Although the energy saving here is more moderate at 11.25%, it still underscores the proposed algorithm's ability to maintain higher efficiency even when operational parameters shift. Turning to the fog layer, a similar trend of enhanced energy efficiency is observed. During Scenario 1, energy consumption drops from 0.433 MJ (traditional) to 0.26 MJ (proposed), equating to a considerable decrease of roughly 40%. In Scenario 2, the proposed system again outperforms its counterpart, recording 0.235 MJ against the traditional system's 0.331 MJ, which corresponds to a reduction of approximately 29%. A closer examination of the overall data reveals two key insights. First, the proposed system consistently outperforms the traditional model across all layers and scenarios, validating its design objectives for energy-conscious computing. Second, both systems exhibit higher energy consumption in Scenario 1 compared to Scenario 2 across both layers, suggesting that Scenario 2 likely involves a lighter computational load or more favorable resource allocation conditions. More importantly, the disparity in energy savings between scenarios indicates that the proposed algorithm's efficiency gains are particularly pronounced under heavier workloads—as evidenced by the dramatic 51.4% cloud-layer reduction in Scenario 1. This highlights the proposed system's robust scalability and its potential for delivering substantial operational cost savings and environmental benefits in data-intensive, high-demand environments.

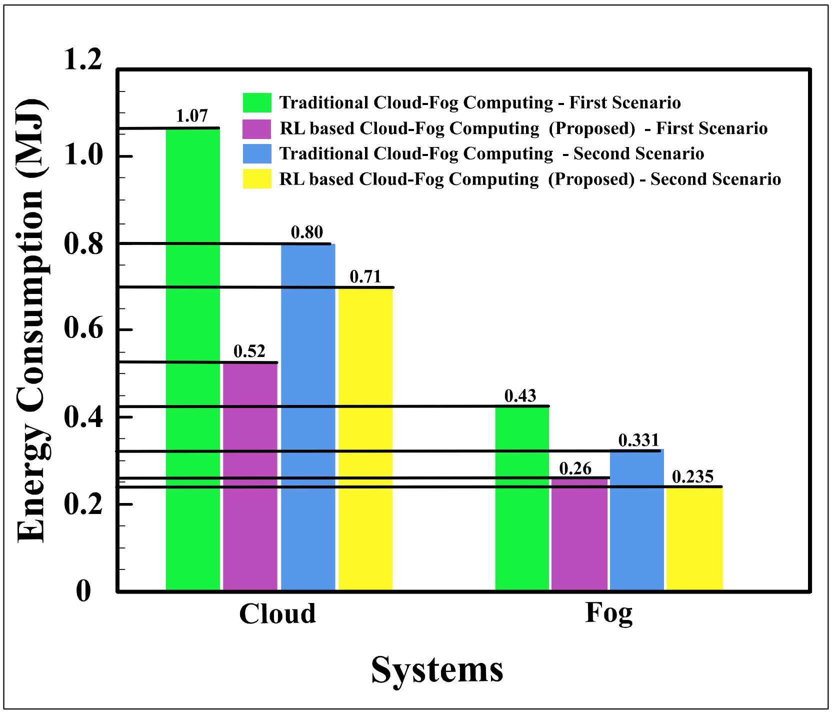

Figure 5. Energy consumption for both scenarios

4. Discussion and Conclusion

The present study evaluated an uncertainty-aware cloud–fog energy management framework based on Deep Deterministic Policy Gradient (DDPG) reinforcement learning for building-integrated photovoltaic systems exposed to two major environmental disturbances: dust accumulation and persistent cloudy weather. Overall, the findings demonstrated that the proposed adaptive architecture outperformed the conventional non-adaptive cloud–fog configuration in transmission latency, processing stability, and computational energy consumption. Under the first scenario, which represented dust accumulation on PV surfaces, cloud-layer transmission time decreased from 186.50 to 130.4, corresponding to a reduction of approximately 30%, while fog-layer transmission time decreased from 27.61 to 12.45, representing an improvement exceeding 54%. Under the second scenario of persistent cloudy weather, cloud-layer transmission time decreased from 169.3 to 110.2, whereas fog-layer latency decreased from 50.90 to 25.07. Thus, the advantages of the DDPG-enabled framework were observed under both slowly evolving soiling uncertainty and more rapidly fluctuating cloud-induced irradiance conditions. These findings indicate that distributing computation hierarchically between fog and cloud layers can substantially improve the responsiveness of PV energy management when environmental conditions continuously alter the state of the physical energy system.

The substantial reduction in transmission latency, particularly at the fog layer, can be explained by the capacity of the proposed architecture to perform time-sensitive processing close to the physical system while reserving computationally intensive policy optimization for the cloud. In the proposed framework, fog nodes perform local sensing, preliminary processing, operational constraint validation, and temporary storage of transition experiences, thereby avoiding the need to repeatedly transfer every low-level control operation to a distant centralized computing resource. This interpretation is consistent with Saoud et al., who demonstrated that intelligent load balancing in cloud–fog smart-grid architectures can reduce response and processing times relative to conventional allocation strategies [22]. Yu et al. similarly showed that coordinated fog and cloud computing can improve smart-grid load balancing, response time, and operating efficiency by positioning computational resources closer to consumers while retaining cloud-level coordination [23]. The present results also agree with Krishnan and Durairaj, who emphasized that fog computing provides low-latency responsiveness while cloud infrastructure offers the processing capacity required for more complex optimization tasks [26]. Accordingly, the large fog-layer latency reductions observed in the present study suggest that the architectural separation of immediate control from global learning is particularly effective for real-time building-integrated PV applications.

The findings concerning processing time provide additional support for this interpretation. In the dust scenario, the conventional architecture displayed sharper and more irregular processing-time spikes, whereas the proposed algorithm generated smoother processing profiles at both the fog and cloud layers. In the cloudy scenario, processing requirements were higher, with approximate average values of 35 ms for the cloud layer and 27 ms for the fog layer compared with approximately 26 ms and 22 ms, respectively, in the first scenario. The traditional system nevertheless continued to exhibit substantially more pronounced fluctuations than the proposed DDPG-based system. In addition, discharge operations produced higher processing requirements than charging operations because they required simultaneous coordination of grid commands and the DC–DC and DC–AC conversion stages. The higher computational burden under cloudy weather is technically plausible because rapidly changing irradiance produces more frequent changes in the state space and therefore requires the control architecture to process and respond to a more dynamic operational environment. Merie and Ahmed showed experimentally that cloudy conditions can strongly alter photovoltaic output [7], while Bonkaney et al. demonstrated that cloud cover can generate immediate output reductions, whereas dust exerts a more cumulative influence on PV energy production [6]. These differences between persistent and transient environmental disturbances help explain why the two scenarios generated different computational patterns in the present analysis.

The ability of the proposed system to maintain smoother processing behavior under variable conditions can also be attributed to the learning characteristics of DDPG. Unlike fixed-rule algorithms, reinforcement-learning agents derive control policies from state–action–reward relationships and can therefore respond dynamically to changes in photovoltaic generation, load, battery status, electricity exchange, and other operating conditions. The theoretical foundation for such performance is closely related to advances in deep neural learning, which permit nonlinear representations of complex system states and relationships [17]. Previous applications of deep reinforcement learning to real-time microgrid energy management have likewise indicated that learning-based controllers can generate effective adaptive decisions in environments characterized by continuously changing renewable generation and demand [16]. Guo et al. further demonstrated the effectiveness of deep reinforcement learning for real-time microgrid energy management under uncertainty [34]. More directly, Mansouri et al. applied deep reinforcement learning within a cloud–fog architecture for real-time multi-microgrid management and showed the suitability of this paradigm for systems exposed to renewable-energy uncertainty [32]. The present findings extend this research direction to building-integrated photovoltaic management by demonstrating that the combination of DDPG and hierarchical computing can improve not only energy dispatch decisions but also the computational characteristics required to implement those decisions in real time.

Energy consumption analysis provided another important finding. In Scenario 1, the traditional cloud layer consumed 1.07 MJ, whereas the proposed framework required only 0.52 MJ, corresponding to a reduction of approximately 51.4%. At the fog layer, energy consumption decreased from 0.433 MJ to 0.26 MJ, or approximately 40%. Under Scenario 2, cloud-layer consumption decreased from 0.80 MJ to 0.71 MJ, representing an 11.25% reduction, whereas fog-layer consumption decreased from 0.331 MJ to 0.235 MJ, representing an approximately 29% reduction. Thus, the DDPG architecture consistently consumed less computational energy than the conventional framework across both scenarios and both computational tiers, although the magnitude of improvement differed considerably by workload and environmental condition. This result is especially important because an energy-management architecture designed for renewable-energy applications should not achieve improved control at the expense of excessive computational energy consumption. The substantial reduction observed under the dust scenario suggests that the adaptive configuration becomes particularly beneficial when sustained environmental disturbances create data-intensive or prolonged computational demands.

These energy-efficiency results correspond closely with previous research on resource allocation and task scheduling in fog–cloud systems. Periasamy et al. found that efficient resource allocation among IoT devices, fog nodes, and resource blocks can significantly improve energy efficiency in fog-IoT environments [25]. Khan et al. likewise showed that machine-learning-based task scheduling can reduce energy consumption while maintaining quality-of-service requirements in IoT-based fog–cloud environments [27]. Mohamed et al. demonstrated that intelligent task scheduling can reduce fog-node energy consumption through optimized resource and routing decisions [28]. Zia et al. further addressed the joint optimization of computation offloading and task scheduling, emphasizing the importance of multi-objective decision-making when both energy expenditure and computational performance must be considered [29]. The present results support these studies but add an energy-domain perspective: computation allocation is not merely an information-technology problem but directly affects the operational sustainability of intelligent renewable-energy systems. By determining when processing should occur locally and when computationally demanding learning should be delegated to the cloud, the proposed framework reduced both communication and processing overhead.

The stronger relative energy savings observed in Scenario 1 are also noteworthy. The proposed system reduced cloud-layer energy consumption by 51.4% under the dusty condition but by only 11.25% under the cloudy condition, while corresponding fog-layer reductions were approximately 40% and 29%. This difference indicates that the benefit of adaptive task management is workload-dependent rather than constant. Under heavier or more sustained workloads, intelligent scheduling has greater opportunity to eliminate redundant computation, reduce unnecessary transmissions, and assign tasks to the most appropriate computational tier. Hemmati and Rahmani showed that data reduction through clustering can decrease redundancy within fog–cloud-enabled IoT infrastructures [24]. Laayati et al. similarly demonstrated the value of integrating forecasting and optimized computation within an edge–fog–cloud framework for energy-intensive applications [30]. Therefore, the particularly strong performance under Scenario 1 may reflect the ability of the proposed framework to exploit persistent state patterns associated with dust accumulation while efficiently coordinating repeated monitoring, forecasting, battery scheduling, and control.

The environmental scenarios themselves also reinforce the importance of uncertainty-aware PV management. Dust-induced soiling is known to cause progressive deterioration in photovoltaic performance. Kazem et al. documented the adverse effect of dust pollutants on PV systems [3], while Khatib et al. experimentally confirmed reductions in multicrystalline module performance following dust deposition [4]. Mani and Pillai characterized dust accumulation as a location- and climate-dependent operational challenge that requires systematic mitigation and maintenance planning [5]. More recently, Yin et al. demonstrated that extreme dust events can substantially reduce regional photovoltaic potential, emphasizing that dust should be incorporated into electricity dispatch and resilience planning rather than viewed exclusively as a maintenance issue [8]. Bhallamudi et al. similarly confirmed the adverse influence of dust and shading on PV module performance [40]. The present findings therefore demonstrate the computational dimension of this established physical problem: environmental degradation of photovoltaic generation also changes the information-processing and decision-making requirements placed on an intelligent EMS.

Cloud uncertainty introduces a different challenge because generation may vary on much shorter timescales. The larger processing requirements observed in the second scenario indicate that rapid solar variability creates a demanding environment for real-time control. This finding supports the need for short-term forecasting methods capable of capturing temporal variations in PV output. Dinesh et al. demonstrated the usefulness of deep learning for short-term multistep photovoltaic-generation forecasting [18], while Amnuaypongsa et al. emphasized prediction intervals as a means of representing uncertainty rather than relying solely on deterministic point forecasts [20]. The inclusion of Prediction Interval Coverage Probability within the present framework is therefore particularly relevant because a controller operating under variable irradiance needs information about both the expected PV output and the uncertainty surrounding that expectation. This approach is compatible with the decision-theoretic principles underlying prediction-interval evaluation, in which coverage and interval width must be considered jointly [19]. Mahala et al. similarly integrated forecasting uncertainty within an edge–fog–cloud microgrid optimization architecture, demonstrating the importance of uncertainty-aware hierarchical energy control [21].

The results also have implications for the integration of storage and power-electronic control. The proposed system does not treat the computational architecture separately from physical energy resources; instead, fog- and cloud-generated decisions ultimately determine battery charging and discharging, inverter operation, grid exchange, and controllable-load behavior. Such coordination is important because battery operation must simultaneously account for state-of-charge constraints, efficiency, degradation, electricity prices, and renewable availability. Eskandari et al. emphasized that battery energy storage has multiple technically and economically distinct functions in microgrid operation and should therefore be coordinated through appropriately designed energy-management strategies [14]. Likewise, robust optimization approaches to microgrid management have shown that uncertainty should be explicitly incorporated into storage and dispatch decisions [15]. At the converter level, effective DC–DC conversion [9], grid-interfaced power conversion [10], and reliable maximum power point tracking under variable or partially shaded conditions [12, 13] remain essential for translating high-level scheduling decisions into physically efficient PV operation.

An additional contribution of the proposed framework is that energy optimization is performed while preserving thermal-comfort considerations rather than treating electricity minimization as the sole objective. The model incorporates adaptive thermal comfort alongside energy expenditure, storage, and system constraints, thereby recognizing that building energy management must serve occupants as well as the electrical network. This principle is consistent with Yao et al., who developed an adaptive predicted mean vote framework to represent the ability of occupants to adjust to changing thermal conditions [37]. Buratti et al. likewise demonstrated the importance of thermal-comfort evaluation in HVAC system assessment and control [35], whereas Ahmed et al. emphasized that thermal comfort, heat resilience, indoor air quality, and energy performance are interdependent objectives in buildings [36]. Consequently, the proposed architecture represents a broader conception of optimality: an intelligent PV building should not merely minimize electrical consumption but should allocate generation, storage, computation, and controllable loads in ways that maintain acceptable occupant conditions.

Taken together, the findings demonstrate that the main advantage of the proposed DDPG-based cloud–fog architecture lies in the simultaneous treatment of environmental uncertainty and computational resource management. The framework reduced transmission latency, stabilized processing behavior, and lowered energy consumption under both dust and cloud uncertainty while retaining a hierarchical decision structure for storage, grid interaction, physical constraints, and thermal comfort. These findings are consistent with broader developments toward resilient renewable-energy systems [1], climate-aware photovoltaic operation [2], intelligent fog-edge processing [39], and IoT-based energy management [31]. They also suggest that future smart-building EMS architectures should be evaluated not only through conventional electrical indicators but through integrated measures of communication latency, computing energy, prediction uncertainty, physical-system robustness, and occupant-oriented performance.

Several limitations should be considered when interpreting the findings. First, the evaluation was based on two predefined environmental scenarios representing dust accumulation and persistent cloudy conditions, and these scenarios cannot encompass the full range of meteorological disturbances experienced by building-integrated PV systems, including simultaneous cloud–dust events, rainfall, extreme temperature, variable wind, and rapidly changing humidity. Second, the performance evaluation was conducted for a particular building-integrated PV, battery, grid, and cloud–fog configuration, so the numerical gains may vary with different hardware capacities, communication technologies, numbers of fog nodes, network congestion levels, storage technologies, electricity tariffs, and building load profiles. Third, the computational evaluation emphasizes transmission time, processing stability, and energy consumption, while other potentially relevant indicators such as packet loss, processor utilization, memory utilization, cybersecurity exposure, hardware failure, battery aging under long-term operation, and lifecycle cost were not comprehensively evaluated. Moreover, although the framework incorporates adaptive thermal comfort and physical operating constraints, actual occupant behavioral responses and long-term field measurements were not used to validate all modeled interactions. These considerations limit the direct generalization of the reported performance improvements to all climates, buildings, and microgrid configurations.

Future studies should evaluate the proposed framework using longer-term field datasets incorporating seasonal variability and simultaneous combinations of dust, cloud cover, temperature, humidity, rainfall, and wind. The architecture should also be tested in multiple buildings and interconnected microgrids to determine how its scalability changes as the number of PV arrays, batteries, fog nodes, IoT devices, and controllable loads increases. Comparative experiments should evaluate DDPG against other reinforcement-learning and optimization approaches, including proximal policy optimization, soft actor–critic, twin-delayed DDPG, multi-agent reinforcement learning, robust optimization, and hybrid metaheuristic-learning methods. Additional research should explicitly quantify prediction-interval calibration, battery degradation, renewable curtailment, carbon emissions, operating costs, thermal-comfort violations, communication reliability, and cybersecurity. Multi-agent extensions could support coordination among neighboring buildings and distributed energy resources, while federated learning could enable collaborative policy improvement without centralized sharing of sensitive building data. Future investigations should also examine hybrid renewable configurations incorporating wind generation, electric vehicles, demand response, and alternative energy-storage technologies.

For practical implementation, smart-building operators should adopt hierarchical energy-management architectures in which time-critical sensing, safety checks, and control functions are located close to physical assets at the fog or edge level, while computationally intensive model training and long-term optimization are assigned to cloud infrastructure. PV facilities in dust-prone regions should integrate real-time soiling monitoring with adaptive maintenance and dispatch scheduling rather than relying exclusively on fixed cleaning intervals. Similarly, buildings exposed to highly variable cloud conditions should combine short-term generation forecasting with uncertainty intervals so that battery dispatch and grid exchange can respond proactively to expected fluctuations. System designers should size fog resources according to expected sensor traffic and control latency requirements, implement fallback control policies when communication or learning components fail, and continuously monitor computational energy use so that the EMS itself remains energy efficient. Finally, deployment decisions should jointly consider renewable generation, battery health, electricity cost, converter limitations, network latency, cybersecurity, and occupant thermal comfort, because optimizing one of these dimensions independently may shift costs or risks to another part of the building energy system.

Authors' Contributions

Authors equally contributed to this article.

Acknowledgments

Authors thank all participants who participate in this study.

Declaration of Interest

The authors report no conflict of interest.

Funding

According to the authors, this article has no financial support.

Ethical Considerations

All procedures performed in this study were under the ethical standards.

References

[1] F. Minelli, D. D'Agostino, V. J. Reddy, and P. Michailidis, "Towards Resilient Cities: Robust Selection of Rooftop Renewable Energy Technologies in Mediterranean Multifamily Buildings," *Energy Engineering: Journal of the Association of Energy Engineers,* vol. 123, no. 6, 2026, doi: 10.32604/ee.2026.074048.

[2] P. Adigun, D. Koji, A. T. Ogunrinde, X. Xue, and P. Ebiendele, "Extreme Weather and Cascading Photovoltaic Power Vulnerabilities under Climate Change," *Sustainable Energy Technologies and Assessments,* vol. 85, p. 104776, 2026, doi: 10.1016/j.seta.2025.104776.

[3] H. A. Kazem, S. Al-Bahri, S. Al-Badi, H. Al-Mahkladi, and A. H. Al-Waeli, "Dust Effect on the Performance of Photovoltaic," *Advanced Materials Research,* vol. 875, pp. 1908-1911, 2014, doi: 10.4028/www.scientific.net/AMR.875-877.1908.

[4] T. Khatib, H. Kazem, K. Sopian, F. Buttinger, W. Elmenreich, and A. S. Albusaidi, "Effect of Dust Deposition on the Performance of Multi-Crystalline Photovoltaic Modules Based on Experimental Measurements," *International Journal of Renewable Energy Research,* vol. 3, no. 4, pp. 850-853, 2013.

[5] M. Mani and R. Pillai, "Impact of Dust on Solar Photovoltaic (PV) Performance: Research Status, Challenges and Recommendations," *Renewable and Sustainable Energy Reviews,* vol. 14, no. 9, pp. 3124-3131, 2010, doi: 10.1016/j.rser.2010.07.065.

[6] A. Bonkaney, S. Madougou, and R. Adamou, "Impacts of Cloud Cover and Dust on the Performance of Photovoltaic

Module in Niamey," *Journal of Renewable Energy,* vol. 2017, no. 1, p. 9107502, 2017, doi: 10.1155/2017/9107502.
[7] F. H. Merie and O. K. Ahmed, "Experimental Assessment of the Performance of the PV/Solar Chimney under the Cloudy Weather," *Results in Engineering,* vol. 23, p. 102605, 2024, doi: 10.1016/j.rineng.2024.102605.
[8] K. Yin, F. Yao, N. Luo, M. Gao, X. Lu, and B. Yi, "Substantial Reduction of Solar Photovoltaic Potential in China by an Extreme Dust Event," *Communications Earth & Environment,* vol. 7, no. 1, p. 44, 2026, doi: 10.1038/s43247-025-03123-1.
[9] X. Hu and C. Gong, "A High Voltage Gain DC-DC Converter Integrating Coupled-Inductor and Diode-Capacitor Techniques," *IEEE Transactions on Power Electronics,* vol. 29, no. 2, pp. 789-800, 2013, doi: 10.1109/TPEL.2013.2257870.
[10] M. A. Barrios, V. Cárdenas, J. M. Sandoval, J. M. Guerrero, and J. C. Vasquez, "A Cascaded DC-AC-AC Grid-Tied Converter for PV Plants with AC-Link," *Electronics,* vol. 10, no. 4, p. 409, 2021, doi: 10.3390/electronics10040409.
[11] F. Moulay, A. Habbati, and A. Lousdad, "The Design and Simulation of a Photovoltaic System Connected to the Grid Using a Boost Converter," *Journal Européen des Systèmes Automatisés,* vol. 55, no. 3, p. 367, 2022, doi: 10.18280/jesa.550309.
[12] M. A. B. Siddique, D. Zhao, A. U. Rehman, K. Ouahada, and H. Hamam, "An Adapted Model Predictive Control MPPT for Validation of Optimum GMPP Tracking under Partial Shading Conditions," *Scientific Reports,* vol. 14, no. 1, p. 9462, 2024, doi: 10.1038/s41598-024-59304-z.
[13] M. N. I. Jamaludin, M. F. N. Tajuddin, T. Younis, S. B. Thanikanti, and M. Khishe, "Hybrid Salp Swarm Maximum Power Point Tracking Algorithm for Photovoltaic Systems in Highly Fluctuating Environmental Conditions," *Scientific Reports,* vol. 15, no. 1, p. 650, 2025, doi: 10.1038/s41598-024-84333-z.
[14] M. Eskandari, A. Rajabi, A. V. Savkin, M. H. Moradi, and Z. Y. Dong, "Battery Energy Storage Systems (BESSs) and the Economy-Dynamics of Microgrids: Review, Analysis, and Classification for Standardization of BESSs Applications," *Journal of Energy Storage,* vol. 55, p. 105627, 2022, doi: 10.1016/j.est.2022.105627.
[15] W. Hu, P. Wang, and H. B. Gooi, "Toward Optimal Energy Management of Microgrids via Robust Two-Stage Optimization," *IEEE Transactions on Smart Grid,* vol. 9, no. 2, pp. 1161-1174, 2016, doi: 10.1109/TSG.2016.2580575.
[16] Y. Ji, J. Wang, J. Xu, X. Fang, and H. Zhang, "Real-Time Energy Management of a Microgrid Using Deep Reinforcement Learning," *Energies,* vol. 12, no. 12, p. 2291, 2019, doi: 10.3390/en12122291.
[17] J. Schmidhuber, "Deep Learning in Neural Networks: An Overview," *Neural Networks,* vol. 61, pp. 85-117, 2015, doi: 10.1016/j.neunet.2014.09.003.
[18] L. P. Dinesh, N. Al Khafaf, and B. McGrath, "A Short Term Multistep Forecasting Model for Photovoltaic Generation Using Deep Learning Model," *Sustainable Operations and Computers,* vol. 6, pp. 34-46, 2025, doi: 10.1016/j.susoc.2024.11.003.
[19] R. L. Winkler, "A Decision-Theoretic Approach to Interval Estimation," *Journal of the American Statistical Association,* vol. 67, no. 337, pp. 187-191, 1972, doi: 10.1080/01621459.1972.10481224.
[20] W. Amnuaypongsa, W. Wangdee, and J. Songsiri, "Neural Network-Based Prediction Interval Estimation with Large Width Penalization for Renewable Energy Forecasting and System Applications," *Energy Conversion and Management: X,* vol. 27, p. 101119, 2025, doi: 10.1016/j.ecmx.2025.101119.
[21] V. R. S. Mahala, A. K. Yadav, D. Saxena, and R. Kumar, "Bi-Level Optimization Framework for Networked Microgrids With Forecasting and Uncertainty Analysis in an Edge-Fog-Cloud Architecture," *IEEE Transactions on Industry Applications,* 2026, doi: 10.1109/TIA.2026.3675195.
[22] A. Saoud and A. Recioui, "Hybrid Algorithm for Cloud-Fog System Based Load Balancing in Smart Grids," *Bulletin of Electrical Engineering and Informatics,* vol. 11, no. 1, pp. 477-487, 2022, doi: 10.11591/eei.v11i1.3450.
[23] D. Yu, Z. Ma, and R. Wang, "Efficient Smart Grid Load Balancing via Fog and Cloud Computing," *Mathematical Problems in Engineering,* vol. 2022, no. 1, p. 3151249, 2022, doi: 10.1155/2022/3151249.
[24] A. Hemmati and A. M. Rahmani, "ClusFC-IoT: A Clustering-Based Approach for Data Reduction in Fog-Cloud-Enabled IoT," *Concurrency and Computation: Practice and Experience,* vol. 36, no. 27, p. e8284, 2024, doi: 10.1002/cpe.8284.
[25] P. Periasamy *et al.*, "ERAM-EE: Efficient Resource Allocation and Management Strategies with Energy Efficiency under Fog-Internet of Things Environments," *Connection Science,* vol. 36, no. 1, p. 2350755, 2024, doi: 10.1080/09540091.2024.2350755.
[26] R. Krishnan and S. Durairaj, "Reliability and Performance of Resource Efficiency in Dynamic Optimization Scheduling Using Multi-Agent Microservice Cloud-Fog on IoT Applications," *Computing,* vol. 106, no. 12, pp. 3837-3878, 2024, doi: 10.1007/s00607-024-01301-1.
[27] A. Khan, F. Ullah, D. Shah, M. H. Khan, S. Ali, and M. Tahir, "EcoTaskSched: A Hybrid Machine Learning Approach for Energy-Efficient Task Scheduling in IoT-Based Fog-Cloud Environments," *Scientific Reports,* vol. 15, no. 1, p. 12296, 2025, doi: 10.1038/s41598-025-96974-9.
[28] A. A. Mohamed *et al.*, "Energy Aware Task Scheduling of IoT Application Using a Hybrid Metaheuristic Algorithm in Cloud Computing," *Computers, Materials & Continua,* vol. 86, no. 3, 2026.
[29] A. Zia *et al.*, "Multi-Objective Enhanced Cheetah Optimizer for Joint Optimization of Computation Offloading and Task Scheduling in Fog Computing," *Computers, Materials & Continua,* vol. 86, no. 3, 2026.
[30] O. Laayati, H. El Hadraoui, A. El Maghraoui, N. Guennouni, M. Mekhfioui, and A. Chebak, "Metaheuristic-Optimized Forecasting in a Smart Edge-Fog-Cloud Energy Management Framework: An Industrial Mining Case Study," *Results in Engineering,* p. 107303, 2025, doi: 10.1016/j.rineng.2025.107303.
[31] M. Rashad, M. S. Abdellatif, and A. H. Rabie, "An Improved Human Evolutionary Optimization Algorithm for Maximizing Green Hydrogen Generation in Intelligent Energy Management System (IEMS)," *Results in Engineering,* vol. 27, p. 105998, 2025, doi: 10.1016/j.rineng.2025.105998.
[32] M. Mansouri, M. Eskandari, Y. Asadi, and A. Savkin, "A Cloud-Fog Computing Framework for Real-Time Energy Management in Multi-Microgrid System Utilizing Deep Reinforcement Learning," *Journal of Energy Storage,* vol. 97, p. 112912, 2024, doi: 10.1016/j.est.2024.112912.
[33] X. Liu *et al.*, "Multi-Agent Primal Dual DDPG Based Reactive Power Optimization of Active Distribution Networks via Graph Reinforcement Learning," *IEEE Internet of Things Journal,* 2025, doi: 10.1109/JIOT.2025.3575445.
[34] C. Guo, X. Wang, Y. Zheng, and F. Zhang, "Real-Time Optimal Energy Management of Microgrid with Uncertainties

Based on Deep Reinforcement Learning," *Energy,* vol. 238, p. 121873, 2022, doi: 10.1016/j.energy.2021.121873.
[35] C. Buratti, P. Ricciardi, and M. Vergoni, "HVAC Systems Testing and Check: A Simplified Model to Predict Thermal Comfort Conditions in Moderate Environments," *Applied Energy,* vol. 104, pp. 117-127, 2013, doi: 10.1016/j.apenergy.2012.11.015.
[36] T. Ahmed, P. Kumar, and L. Mottet, "Natural Ventilation in Warm Climates: The Challenges of Thermal Comfort, Heatwave Resilience and Indoor Air Quality," *Renewable and Sustainable Energy Reviews,* vol. 138, p. 110669, 2021, doi: 10.1016/j.rser.2020.110669.
[37] R. Yao, B. Li, and J. Liu, "A Theoretical Adaptive Model of Thermal Comfort-Adaptive Predicted Mean Vote (aPMV)," *Building and Environment,* vol. 44, no. 10, pp. 2089-2096, 2009, doi: 10.1016/j.buildenv.2009.02.014.
[38] C. Chellaswamy, R. Ganesh Babu, and A. Vanathi, "A Framework for Building Energy Management System with Residence Mounted Photovoltaic," *Building Simulation,* vol. 14, no. 4, pp. 1031-1046, 2021, doi: 10.1007/s12273-020-0735-x.
[39] F. Al-Quayed, "AI-Powered Anomaly Detection and Cybersecurity in Healthcare IoT with Fog-Edge," *Computer Modeling in Engineering & Sciences (CMES),* vol. 146, no. 1, p. 1, 2026, doi: 10.32604/cmes.2025.074799.
[40] R. Bhallamudi, S. Kumarasamy, and C. Sundarabalan, "Effect of Dust and Shadow on Performance of Solar Photovoltaic Modules: Experimental Analysis," *Energy Engineering: Journal of the Association of Energy Engineers,* vol. 118, no. 6, p. 1827, 2021, doi: 10.32604/EE.2021.016798.